Article

Selecting Topology and Connectivity through Metal-Directed Macrocyclization Reactions: A Square Planar Palladium [2]Catenate and Two Noninterlocked Isomers

Anne-Marie L. Fuller, David A. Leigh, Paul J. Lusby, Alexandra M. Z. Slawin, and D. Barney Walker

J. Am. Chem. Soc., **2005**, 127 (36), 12612-12619• DOI: 10.1021/ja053005a • Publication Date (Web): 17 August 2005

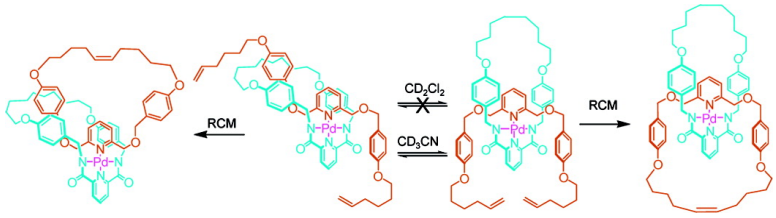

More About This Article

Additional resources and features associated with this article are available within the HTML version:

- Supporting Information
- Links to the 22 articles that cite this article, as of the time of this article download
- Access to high resolution figures
- Links to articles and content related to this article
- Copyright permission to reproduce figures and/or text from this article

View the Full Text HTML

J|A|C|S
ARTICLES
Published on Web 08/17/2005

Selecting Topology and Connectivity through Metal-Directed Macrocyclization Reactions: A Square Planar Palladium [2]Catenate and Two Noninterlocked Isomers

Anne-Marie L. Fuller,[†] David A. Leigh,*[,†] Paul J. Lusby,[†] Alexandra M. Z. Slawin,[‡] and D. Barney Walker[†]

Contribution from the School of Chemistry, University of Edinburgh, The King's Buildings, West Mains Road, Edinburgh EH9 3JJ, United Kingdom, and the School of Chemistry, University of St. Andrews, Purdie Building, St. Andrews, Fife, KY16 9ST, United Kingdom

Received May 8, 2005; E-mail: David.Leigh@ed.ac.uk

Abstract: We report the synthesis of a [2]catenate using a square planar palladium(II) template, together with two isomers of the interlocked structure: a single tetradentate macrocycle that adopts a "figure of eight" conformation to encapsulate the metal and a complex in which the two macrocycles of the catenane are not interlocked. The three isomers can each be selectively formed depending on how the building blocks are assembled and cyclized. Olefin metathesis of both building blocks while they are attached to the metal gives the single large macrocycle in 77% yield. Cyclizing the monodentate unit prior to attaching both ligands to the metal gives the [2]catenate in 78% yield. Preforming the tridentate macrocycle produces a complex in two atropisomeric forms—threaded and nonthreaded—in a 2:3 ratio, which do not interconvert in dichloromethane at room temperature over 7 days. RCM of the nonthreaded atropisomer affords the complex with two noninterlocked macrocyclic ligands; RCM of the threaded atropisomer generates the topologically isomeric [2]catenate. Heating the acyclic atropisomers in acetonitrile provides a mechanism for their interconversion via ligand exchange, allowing the threaded:nonthreaded ratio to be varied from 2:3 to 8:1. All three fully ring-closed complexes were characterized unambiguously by ^{1}H NMR spectroscopy and X-ray crystallography. As far as we are aware, this is the first time such a set of three formal topological and constitutional isomers has been described.

Introduction

The use of transition metal ions to direct the synthesis of interlocked architectures remains among the most efficient strategies available.[1−8] In addition to exploiting reversible coordination chemistry to deliver high yields of thermodynamically privileged catenanes incorporating metals in their ring frameworks,[2] catenates—metal complexes of interlocked organic macrocyclic ligands—can be formed through metal template macrocyclization reactions. However, while the use of tetrahedral copper(I) geometry to hold bidentate ligands in an orientation suitable for subsequent interlocking macrocyclization reactions has been extensively developed over a 20 year period,[3−8] the transposition of this basic concept to other coordination modes has been slow to develop. Although Sokolov alluded to the possibility of using octahedral ions to template catenane synthesis as early as 1973,[9] attempts to prepare interlocked architectures in this way initially met with limited success,[2c,10] and it is only recently[11] that efficient synthetic routes based on octahedral coordination have been developed. There is also a single example[12] of five-coordinate zinc(II) being used to direct the formation of a [2]catenate and a remarkable crown ether-threaded organometallic catenate templated about a magnesium atom that also forms part of one ring.[13]

At first sight, the use of a template strategy to produce interlocked macrocyclic ligands for metals with a square planar coordination geometry might appear somewhat counter-intuitive. Square planar coordination obviously involves a 2D donor set, while interlocking of the two rings requires two crossing points (one positive, one negative[14]) necessitating control over the nature of covalent bond formation in the third dimension. However, by using a tridentate−monodentate ligand combination, the relative orientation of the ligands coordinated to the metal can be varied (formally by rotation about the monodentate ligand−metal bond), and therefore, in principle, systems can be designed to extend above and below the plane of the square planar coordination mode and direct a subsequent ring closure reaction. Indeed, there are several examples[15,16] of the orthogonal alignment of organic fragments using such a "3 + 1" donor set of ligands, and we recently found that it was possible to exploit this effect to form a mechanically interlocked structure (Scheme 1).[17] Through a combination of electronic and steric factors, the square planar palladium holds the monodentate 2,6-

[†] University of Edinburgh.
[‡] University of St. Andrews.

(1) For reviews on interlocked molecules assembled about transition metal templates, see: (a) Sauvage, J.-P.; Dietrich-Buchecker, C. *Molecular Catenanes, Rotaxanes and Knots*; Wiley-VCH: Weinheim, Germany, 1999. (b) Hubin, T. J.; Busch, D. H. *Coord. Chem. Rev.* **2000**, *200−202*, 5−52. (c) Collin, J.-P.; Dietrich-Buchecker, C.; Gaviña, P.; Jimenez-Molero, M. C.; Sauvage, J.-P. *Acc. Chem. Res.* **2001**, *34*, 477−487. (d) Menon, S. K.; Guha, T. B.; Agrawal, Y. K. *Rev. Inorg. Chem.* **2004**, *24*, 97−133. (e) Cantrill, S. J.; Chichak, K. S.; Peters, A. J.; Stoddart, J. F. *Acc. Chem. Res.* **2005**, *38*, 1−9.

10.1021/ja053005a CCC: $30.25

dimethyleneoxypyridine thread orthogonal to a bis-olefin-terminated tridentate benzylic amide macrocycle precursor such that cyclization by ring closing olefin metathesis (RCM) results in a [2]rotaxane in 77% yield.

However, extending this strategy to catenane synthesis is not straightforward. Even though oligomer and polymer formation could be minimized by metal chelation of the acyclic building blocks, a double macrocyclization strategy could produce three different isomeric products (**1**−**3**, Scheme 2), and even preforming one of the rings prior to attaching the building blocks to the metal could still afford either the interlocked (**1**) or noninterlocked (**3**) complex. Therefore we explored several potential routes to a square planar coordination [2]catenate, varying the sequence that the rings were cyclized and whether or not the building blocks were attached to the metal prior to macrocyclization. Remarkably, it proved possible to find synthetic routes to each of the isomers **1**−**3** shown in Scheme 2.

Scheme 1. Palladium(II)-Directed Synthesis of a [2]Rotaxane[17]

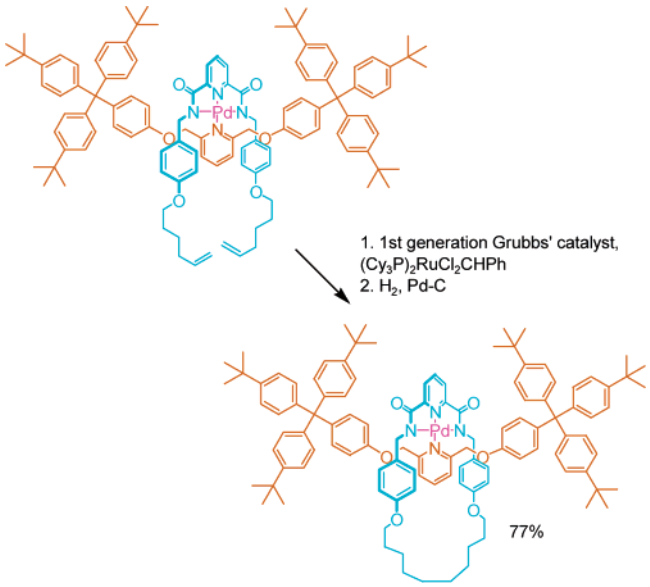

Results and Discussion

Route I: Simultaneous Metal-Directed Olefin Metathesis of L1 and L2. The first route investigated was the possible

(2) (a) Fujita, M.; Ibukuro, F.; Hagihara, H.; Ogura, K. *Nature* **1994**, *367*, 720−723. (b) Fujita, M.; Ibukuro, F.; Yamaguchi, K.; Ogura, K. *J. Am. Chem. Soc.* **1995**, *117*, 4175−4176. (c) Piguet, C.; Bernardinelli, G.; Williams, A. F.; Bocquet, B. *Angew. Chem., Int. Ed. Engl.* **1995**, *34*, 582−584. (d) Mingos, D. M. P.; Yau, J.; Menzer, S.; Williams, D. J. *Angew. Chem., Int. Ed. Engl.* **1995**, *34*, 1894−1895. (e) Fujita, M.; Ogura, K. *Bull. Chem. Soc. Jpn.* **1996**, *69*, 1471−1482. (f) Fujita, M.; Ogura, K. *Coord. Chem. Rev.* **1996**, *148*, 249−264. (g) Fujita, M.; Ibukuro, F.; Seki, H.; Kamo, O.; Imanari, M.; Ogura, K. *J. Am. Chem. Soc.* **1996**, *118*, 899−900. (h) Cárdenas, D. J.; Sauvage, J.-P. *Inorg. Chem.* **1997**, *36*, 2777−2783. (i) Cárdenas, D. J.; Gaviña, P.; Sauvage, J.-P. *J. Am. Chem. Soc.* **1997**, *119*, 2656−2664. (j) Fujita, M.; Aoyagi, M.; Ibukuro, F.; Ogura, K.; Yamaguchi, K. *J. Am. Chem. Soc.* **1998**, *120*, 611−612. (k) Whang, D.; Park, K.-M.; Heo, J.; Kim, K. *J. Am. Chem. Soc.* **1998**, *120*, 4899−4900. (l) Try, A. C.; Harding, M. M.; Hamilton, D. G.; Sanders, J. K. M. *J. Chem. Soc., Chem. Commun.* **1998**, 723−724. (m) Fujita, M.; Fujita, N.; Ogura, K.; Yamaguchi, K. *Nature* **1999**, *400*, 52−55. (n) Fujita, M. *Acc. Chem. Res.* **1999**, *32*, 53−61. (o) Dietrich-Buchecker, C.; Geum, N.; Hori, A.; Fujita, M.; Sakamoto, S.; Yamaguchi, K.; Sauvage, J.-P. *Chem. Commun.* **2001**, 1182−1183. (p) Padilla-Tosta, M. E.; Fox, O. D.; Drew, M. G. B.; Beer, P. D. *Angew. Chem., Int. Ed.* **2001**, *40*, 4235−4239. (q) Park, K.-M.; Kim, S.-Y.; Heo, J.; Whang, D.; Sakamoto, S.; Yamaguchi, K.; Kim, K. *J. Am. Chem. Soc.* **2002**, *124*, 2140−2147. (r) Kim, K. *Chem. Soc. Rev.* **2002**, *31*, 96−107. (s) McArdle, C. P.; Irwin, M. J.; Jennings, M. C.; Vittal, J. J.; Puddephatt, R. J. *Chem.—Eur. J.* **2002**, *8*, 723−734. (t) McArdle, C. P.; Van, S.; Jennings, M. C.; Puddephatt, R. J. *J. Am. Chem. Soc.* **2002**, *124*, 3959−3965. (u) Dietrich-Buchecker, C.; Colasson, B.; Fujita, M.; Hori, A.; Geum, N.; Sakamoto, S.; Yamaguchi, K.; Sauvage, J.-P. *J. Am. Chem. Soc.* **2003**, *125*, 5717−5725. (v) Hori, A.; Kataoka, H.; Akasaka, A.; Okano, T.; Fujita, M. *J. Polym. Sci. Part A: Polym. Chem.* **2003**, *41*, 3478−3485. (w) Mohr, F.; Eisler, D. J.; McArdle, C. P.; Atieh, K.; Jennings, M. C.; Puddephatt, R. J. *J. Organomet. Chem.* **2003**, *670*, 27−36. (x) Mohr, F.; Jennings, M. C.; Puddephatt, R. J. *Eur. J. Inorg. Chem.* **2003**, 217−223. (y) Colasson, B. X.; Sauvage, J.-P. *Inorg. Chem.* **2004**, *43*, 1895−1901. (z) Hori, A.; Yamashita, K.; Kusukawa, T.; Akasaka, A.; Biradha, K.; Fujita, M. *Chem. Commun.* **2004**, 1798−1799. (aa) Burchell, T. J.; Eisler, D. J.; Puddephatt, R. J. *Dalton Trans.* **2005**, 268−272. (bb) Wong, W. W. H.; Cookson, J.; Evans, E. A. L.; McInnes, E. J. L.; Wolowska, J.; Maher, J. P.; Bishop, P.; Beer, P. D. *Chem. Commun.* **2005**, 2214−2216.

(3) For catenates assembled around a tetrahedral four-coordinate Cu(I) template, see: (a) Dietrich-Buchecker, C. O.; Sauvage, J.-P.; Kintzinger, J.-P. *Tetrahedron Lett.* **1983**, *24*, 5095−5098. (b) Dietrich-Buchecker, C. O.; Sauvage, J.-P.; Kern, J.-M. *J. Am. Chem. Soc.* **1984**, *106*, 3043−3045. (c) Cesario, M.; Dietrich-Buchecker, C. O.; Guilhem, J.; Pascard, C.; Sauvage, J.-P. *J. Chem. Soc., Chem. Commun.* **1985**, 244−247. (d) Dietrich-Buchecker, C. O.; Guilhem, J.; Khemiss, A. K.; Kintzinger, J.-P.; Pascard, C.; Sauvage, J.-P. *Angew. Chem., Int. Ed. Engl.* **1987**, *26*, 661−663. (e) Dietrich-Buchecker, C. O.; Edel, A.; Kintzinger, J.-P.; Sauvage, J.-P. *Tetrahedron* **1987**, *43*, 333−344. (f) Jørgensen, T.; Becher, J.; Chambron, J.-C.; Sauvage, J.-P. *Tetrahedron Lett.* **1994**, *35*, 4339−4342. (g) Kern, J.-M.; Sauvage, J.-P.; Weidmann, J.-L. *Tetrahedron* **1996**, *52*, 10921−10934. (h) Kern, J.-M.; Sauvage, J.-P.; Weidmann, J.-L.; Armaroli, N.; Flamigni, L.; Ceroni, P.; Balzani, V. *Inorg. Chem.* **1997**, *36*, 5329−5338. (i) Mohr, B.; Weck, M.; Sauvage, J.-P.; Grubbs, R. H. *Angew. Chem., Int. Ed. Engl.* **1997**, *36*, 1308−1310. (j) Amabilino, D. B.; Sauvage, J.-P. *New J. Chem.* **1998**, *22*, 395−409. (k) Weidmann, J.-L.; Kern, J.-M.; Sauvage, J.-P.; Muscat, D.; Mullins, S.; Köhler, W.; Rosenauer, C.; Räder, H. J.; Martin, K.; Geerts, Y. *Chem.—Eur. J.* **1999**, *5*, 1841−1851. (l) Raehm, L.; Hamann, C.; Kern, J.-M.; Sauvage, J.-P. *Org. Lett.* **2000**, *2*, 1991−1994.

(4) For chiral [2]catenates assembled around tetrahedral four-coordinate Cu(I) templates, see: (a) Chambron, J.-C.; Mitchell, D. K.; Sauvage, J.-P. *J. Am. Chem. Soc.* **1992**, *114*, 4625−4631. (b) Kaida, Y.; Okamoto, Y.; Chambron, J.-C.; Mitchell, D. K.; Sauvage, J.-P. *Tetrahedron Lett.* **1993**, *34*, 1019−1022.

(5) For doubly interlocked [2]catenates assembled around tetrahedral four-coordinate Cu(I) templates, see: Nierengarten, J.-F.; Dietrich-Buchecker, C. O.; Sauvage, J.-P. *J. Am. Chem. Soc.* **1994**, *116*, 375−376.

(6) For rotaxanes assembled around a tetrahedral four-coordinate Cu(I) template, see: (a) Wu, C.; Lecavalier, P. R.; Shen, Y. X.; Gibson, H. W. *Chem. Mater.* **1991**, *3*, 569−572. (b) Chambron, J.-C.; Heitz, V.; Sauvage, J.-P. *J. Chem. Soc., Chem. Commun.* **1992**, 1131−1133. (c) Chambron, J.-C.; Heitz, V.; Sauvage, J.-P. *J. Am. Chem. Soc.* **1993**, *115*, 12378−12384. (d) Diederich, F.; Dietrich-Buchecker, C.; Nierengarten, J.-F.; Sauvage, J.-P. *J. Chem. Soc., Chem. Commun.* **1995**, 781−782. (e) Cárdenas, D. J.; Gaviña, P.; Sauvage, J.-P. *Chem. Commun.* **1996**, 1915−1916. (f) Solladié, N.; Chambron, J.-C.; Dietrich-Buchecker, C. O.; Sauvage, J.-P. *Angew. Chem., Int. Ed. Engl.* **1996**, *35*, 906−909. (g) Armaroli, N.; Diederich, F.; Dietrich-Buchecker, C. O.; Flamigni, L.; Marconi, G.; Nierengarten, J.-F.; Sauvage, J.-P. *Chem.—Eur. J.* **1998**, *4*, 406−416. (h) Armaroli, N.; Balzani, V.; Collin, J.-P.; Gaviña, P.; Sauvage, J.-P.; Ventura, B. *J. Am. Chem. Soc.* **1999**, *121*, 4397−4408. (i) Solladié, N.; Chambron, J.-C.; Sauvage, J.-P. *J. Am. Chem. Soc.* **1999**, *121*, 3684−3692. (j) Weber, N.; Hamann, C.; Kern, J.-M.; Sauvage, J.-P. *Inorg. Chem.* **2003**, *42*, 6780−6792. (k) Poleschak, I.; Kern, J.-M.; Sauvage, J.-P. *Chem. Commun.* **2004**, 474−476. (l) Kwan, H. P.; Swager, T. M. *J. Am. Chem. Soc.* **2005**, *127*, 5902−5909.

(7) For a rotaxane dimer assembled around tetrahedral four-coordinate Cu(I) templates, see: Jiménez, M. C.; Dietrich-Buchecker, C.; Sauvage, J.-P. *Angew. Chem., Int. Ed.* **2000**, *39*, 3284−3287.

(8) For knots assembled around tetrahedral four-coordinate Cu(I) templates, see: (a) Dietrich-Buchecker, C. O.; Sauvage, J.-P. *Angew. Chem., Int. Ed. Engl.* **1989**, *28*, 189−192. (b) Dietrich-Buchecker, C. O.; Nierengarten, J.-F.; Sauvage, J.-P. *Tetrahedron Lett.* **1992**, *33*, 3625−3628. (c) Dietrich-Buchecker, C. O.; Sauvage, J.-P.; Kintzinger, J.-P.; Maltese, P.; Pascard, C.; Guilhem, J. *New. J. Chem.* **1992**, *16*, 931−942. (d) Dietrich-Buchecker, C. O.; Sauvage, J.-P.; De Cian, A.; Fischer, J. *J. Chem. Soc., Chem. Commun.* **1994**, 2231−2232. (e) Perret-Aebi, L.-E.; von Zelewsky, A.; Dietrich-Buchecker, C.; Sauvage, J.-P. *Angew. Chem. Int. Ed.* **2004**, *43*, 4482−4485.

(9) (a) Sokolov V. I. *Usp. Khim.* **1973**, *42*, 1037−1059; *Russ. Chem. Rev. (Engl. Transl.)* **1973**, *42*, 452−463. For later discussions on possible strategies to catenates based on octahedral metal templates, see: (b) Busch, D. H. *J. Inclusion Phenom. Mol. Recognit.* **1992**, *12*, 389−395. (c) Gerbeleu, N. V.; Arion, V. B.; Burgess, J. *Template Synthesis of Macrocyclic Compounds*; Wiley-VCH: Weinheim, Germany 1999; and ref 1b.

(10) Belfrekh, N.; Dietrich-Buchecker, C.; Sauvage, J.-P. *Inorg. Chem.* **2000**, *39*, 5169−5172.

(11) (a) Leigh, D. A.; Lusby, P. J.; Teat, S. J.; Wilson, A. J.; Wong, J. K. Y.; *Angew. Chem., Int. Ed.* **2001**, *40*, 1538−1543. (b) Mobian, P.; Kern, J.-M.; Sauvage, J.-P. *J. Am. Chem. Soc.* **2003**, *125*, 2016−2017. (c) Arico, F.; Mobian, P.; Kern, J.-M.; Sauvage, J.-P. *Org. Lett.* **2003**, *5*, 1887−1890. (d) Hogg, L.; Leigh, D. A.; Lusby, P. J.; Morelli, A.; Parsons, S.; Wong, J. K. Y. *Angew. Chem., Int. Ed.* **2004**, *43*, 1218−1221. (e) Mobian, P.; Kern, J.-M.; Sauvage, J.-P. *Angew. Chem., Int. Ed.* **2004**, *43*, 2392−2395. (f) Chambron, J.-C.; Collin, J.-P.; Heitz, V.; Jouvenot, D.; Kern, J.-M.; Mobian, P.; Pomeranc, D.; Sauvage, J.-P. *Eur. J. Org. Chem.* **2004**, 1627−1638.

Scheme 2. Schematic Representation of the Three Isomers that Result from Synchronous or Simultaneous Metal-Directed Cyclization of Two Acyclic Building Blocks[a]

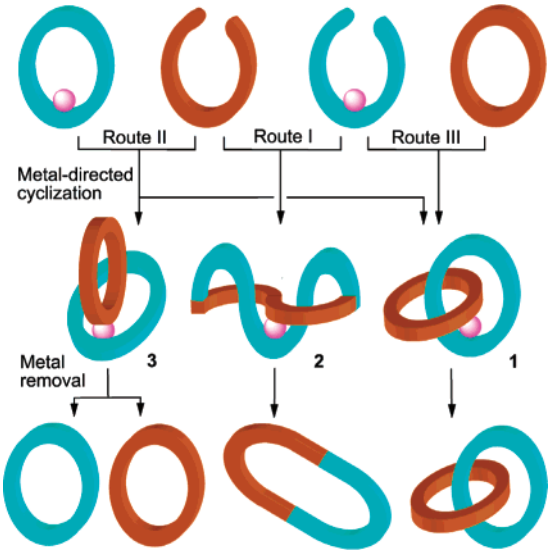

[a] Homodimerization is avoided by using one tridentate ligand (blue) and one monodentate ligand (orange) and a metal with a preferred square planar coordination geometry. Other possible reaction products could potentially include knots (although knotted isomers of **1**−**3** are easily precluded by limiting the size of the building blocks) and higher cyclic, catenated and knotted oligomers and polymers resulting from the condensation of more than just one of each building block (minimized by carrying out the cyclization reactions at high dilution).

double macrocyclization of the tridentate (H_2**L1**) and monodentate (**L2**) building blocks, with both ligands already coordinated to a square planar metal, **L1**Pd**L2** (Scheme 3, Route I). The monodentate ligand **L2** was prepared in two steps from 4-hydroxybenzyl alcohol (see Supporting Information) and when combined with the known **L1**Pd(CH_3CN) complex in dichloromethane, this provided the tetra-terminal olefin complex, **L1**Pd**L2**, in 93% yield (Scheme 3, ii). ^{1}H NMR confirms the exchange of the acetonitrile ligand for **L2** (Figure 1a,b; note the upfield shift of the aromatic resonances of **L1** (H_E and H_F) by 0.8 and 0.2 ppm, respectively, due to stacking with the pyridine group of **L2**).

Subjecting **L1**Pd**L2** to RCM using the first-generation Grubbs' olefin metathesis catalyst,[18] followed by hydrogenation of the resulting internal double bond (Scheme 3, iii), gave a single species in 75% isolated yield for the two steps. FAB mass spectrometry confirmed that the complex had the molecular weight (m/z = 1110, MH^+) necessary to be one of the isomers **1**−**3**, and the ^{1}H NMR spectrum (Figure 1c) showed significant differences to **L1**Pd**L2**, most notably in the region of 2.5−5.5 ppm, indicating that some change in orientation of the building blocks had occurred upon RCM. Treatment of the complex with potassium cyanide (Scheme 3, iv) gave a single organic compound (confirmed by mass spectrometry and ^{1}H NMR), ruling out the possibility that the product of the RCM was the two noninterlocked ring isomer, **3**; that is, the product of Route I could not be **L4**Pd**L5**.

The ^{1}H NMR spectrum (Figure 2c) of the demetalated structure did not show the shielding effects characteristic of benzylic amide macrocycle interlocked systems, the chemical shifts being virtually identical to the independently prepared free ligands, H_2**L4** and **L5** (Figure 2a and d, respectively). This suggested that the ligand isomer formed from Route I was probably H_2**L3**, the single large macrocycle (**2**) resulting from intercomponent metathesis between the **L1** and **L2** olefin groups. This assignment was confirmed when single crystals suitable for X-ray crystallography were grown from slow cooling of a hot, saturated acetonitrile solution of the complex formed by Route I. The solid state structure (Figure 3) shows the tetradentate 58-membered single macrocycle satisfying the square planar coordination geometry of the palladium, with the tridentate 2,6-dicarboxamidopyridine moiety held orthogonally to the monodentate 2,6-bis(oxymethylene)pyridine group. This results in twisting of the macrocycle, providing a single crossover point in a distinctive figure-of-eight conformation (Figure 3b). Although rare, this shape is not unique among coordination complexes of large flexible macrocycles, with other examples—based on octahedral metals—reported by the groups of Sauvage (a 58-membered hexadentate bis-terpy macrocycle bound to iron(II))[10] and Busch (a 40-membered ring coordinating to nickel(II) via 2,6-diiminopyridine groups).[19] In all cases, the metal ion provides the crossover point, imposing helical chirality on what would otherwise be intrinsically achiral macrocycles (for **L3**Pd, both enantiomers are observed in the unit cell). Re-examination of the ^{1}H NMR spectrum (Figure 1c) reveals that the ring conformation of **L3**Pd is conserved from the solid state to solution. The low (C_2) symmetry results in the individual protons of the H_D, H_c, and H_d methylene groups (H_D, $H_{D'}$, H_c, $H_{c'}$, H_d, and $H_{d'}$) being held in diastereotopic environments; the magnitude of the splittings following their proximity to the crossover point (H_D and $H_{D'}$ are split by nearly 2.5 ppm, H_c and $H_{c'}$ by 1.0 ppm, and H_d and $H_{d'}$ by just 0.4 ppm). Interestingly, the aromatic region of **L3**Pd is virtually identical to that of **L1**Pd**L2** (Figure 1b), suggesting that while the alkyl residues may be mobile, the rest of the acyclic precursor complex is well-organized for intercomponent olefin metathesis.

Since the attempted simultaneous double macrocyclization strategy had given rise to intercomponent bond formation, we sought to exclude this possibility[20] by preforming one or the other of the rings prior to the second, metal-directed, cyclization reaction (Scheme 3, Routes II and III).

Route II: Metal-Directed RCM of L2. Tridentate macrocycle H_2**L4** was prepared in 57% yield by treatment of 2,6-

(12) Hamann, C.; Kern, J.-M.; Sauvage, J.-P. *Inorg. Chem.* **2003**, *42*, 1877−1883.
(13) Gruter, G.-J. M.; de Kanter, F. J. J.; Markies, P. R.; Nomoto, T.; Akkerman, O. S.; Bickelhaupt, F. *J. Am. Chem. Soc.* **1993**, *115*, 12179−12180.
(14) Flapan, E. A Knot Theoretic Approach to Molecular Chirality. In *Molecular Catenanes, Rotaxanes and Knots*; Sauvage, J.-P., Dietrich-Buchecker, C., Eds.; Wiley-VCH: Weinheim, Germany, 1999; pp 7−35.
(15) (a) Kickham, J. E.; Loeb, S. J. *Inorg. Chem.* **1994**, *33*, 4351−4359. (b) Kickham, J. E.; Loeb, S. J.; Murphy, S. L. *Chem.—Eur. J.* **1997**, *3*, 1203−1213.
(16) Hamann, C.; Kern, J.-M.; Sauvage, J.-P. *Dalton. Trans.* **2003**, 3770−3775.
(17) (a) Fuller, A.-M.; Leigh, D. A.; Lusby, P. J.; Oswald, I. D. H.; Parsons, S.; Walker, D. B. *Angew. Chem., Int. Ed.* **2004**, *43*, 3914−3918. (b) Furusho, Y.; Matsuyama, T.; Takata, T.; Moriuchi, T.; Hirao, T. *Tetrahedron Lett.* **2004**, *45*, 9593−9597. (c) Leigh, D. A.; Lusby, P. J.; Slawin, A. M. Z.; Walker, D. B. *Angew. Chem., Int. Ed.* **2005**, *44*, 4557−4564.
(18) (a) Schwab, P.; France, M. B.; Ziller, J. W.; Grubbs, R. H. *Angew. Chem., Int. Ed. Engl.* **1995**, *34*, 2039−2041. (b) Grubbs, R. H.; Miller, S. J.; Fu, G. C. *Acc. Chem. Res.* **1995**, *28*, 446−452.
(19) Vance, A. L.; Alcock, N. W.; Busch, D. H.; Heppert, J. A. *Inorg. Chem.* **1997**, *36*, 5132−5134.
(20) At least as long as the RCM reaction is not under thermodynamic control. However, metathesis of internal olefins is generally much slower than that of terminal olefins. See, for example: Kidd, T. J.; Leigh, D. A.; Wilson, A. J. *J. Am. Chem. Soc.* **1999**, *121*, 1599−1600.

Scheme 3 [a]

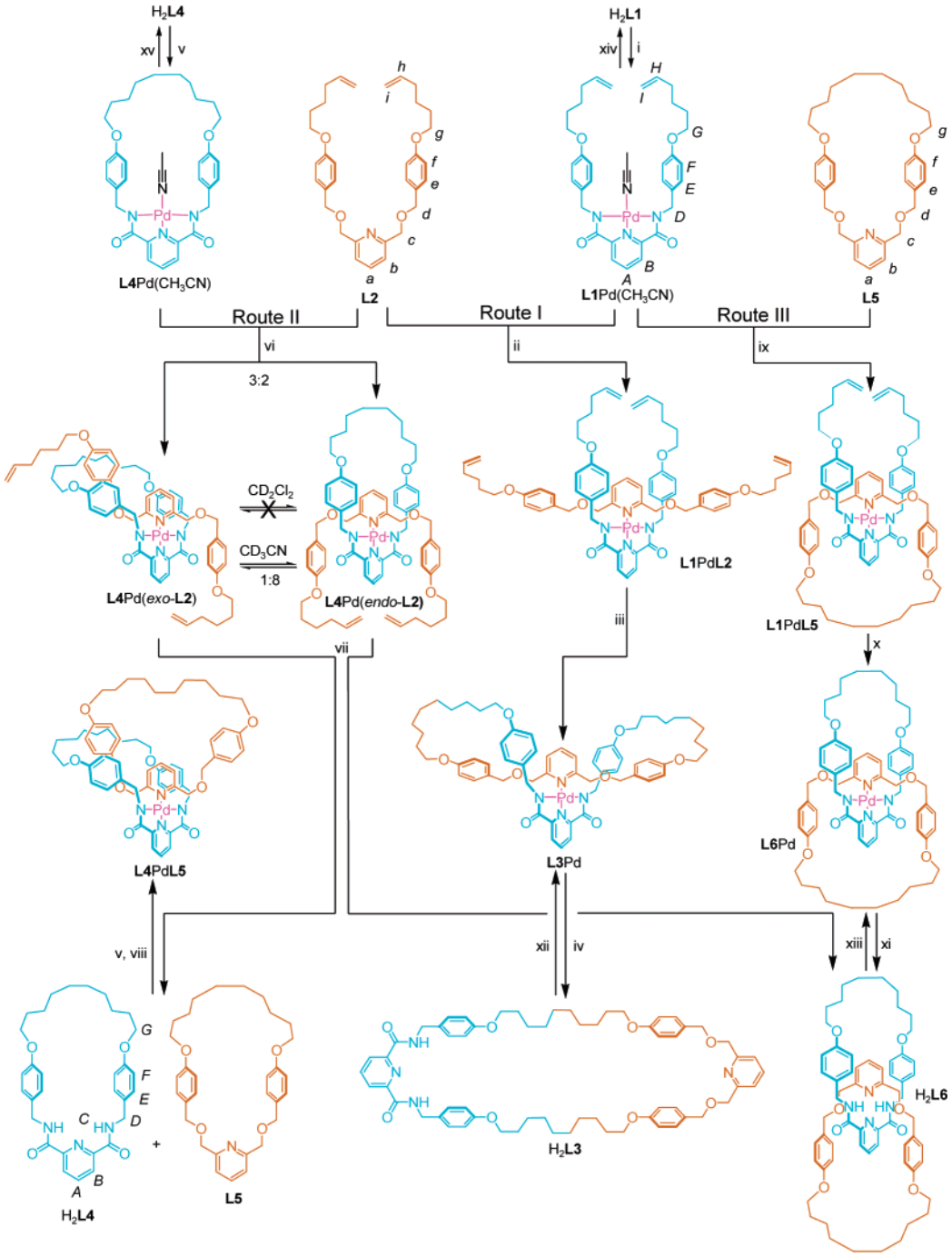

[a] Reagents and conditions: (i) $Pd(OAc)_2$, CH_3CN, 1 h, 76%; (ii) CH_2Cl_2, 1 h, 93%; (iii) a. first-generation Grubbs' catalyst $(Cy_3P)_2Cl_2RuCHPh$, 0.2 equiv, CH_2Cl_2, 20 h; b. H_2, Pd−C, THF, 4 h, 75% (over two steps); (iv) KCN, MeOH, CH_2Cl_2, 20 °C, 1 h and then 40 °C, 0.5 h, 94%; (v) $Pd(OAc)_2$, CH_3CN, 1 h, 93%; (vi) CH_2Cl_2, 1 h, a 3:2 ratio of **L4**Pd(*exo*-**L2**):**L4**Pd(*endo*-**L2**), isolated in 89% yield; (vii) a. first-generation Grubbs' catalyst (0.1 equiv), CH_2Cl_2, 22 h; b. H_2 (50 bar), Pd EnCat, THF, 18 h; c. KCN, MeOH, CH_2Cl_2, 20 °C, 1 h and then 40 °C, 0.5 h, H_2**L4**, **L5**, and H_2**L6** (25% over three steps); (viii) part (v) and then CH_2Cl_2, 1 h, 78%; (ix) CH_2Cl_2, 1 h, 69%; (x) a. first-generation Grubbs' catalyst (0.1 equiv), CH_2Cl_2, 22 h; b. H_2, Pd−C, THF, 4 h, 78% (over two steps); (xi) KCN, MeOH, CH_2Cl_2, 20 °C, 1 h and then 40 °C, 0.5 h, 97%; (xii) $Pd(OAc)_2$, CH_3CN, 60 °C, 4 h, 85%; (xiii) $Pd(OAc)_2$, CH_3CN, 60 °C, 4 h, 79%; (xiv) KCN, MeOH, CH_2Cl_2, 20 °C, 1 h and then 40 °C, 0.5 h, 98%; (xv) KCN, MeOH, CH_2Cl_2, 20 °C, 1 h and then 40 °C, 0.5 h, 95%.

pyridinedicarbonyl dichloride with the appropriate diamine under high dilution conditions (see Supporting Information). Subsequent complexation with palladium(II) acetate afforded **L4**Pd(CH_3CN) (93%, Scheme 3, v). Threading of **L2** through the cavity of **L4**Pd(CH_3CN) via the substitution of the coordinated acetonitrile was attempted by simple mixing of the two in dichloromethane at room temperature (Scheme 3, vi). While mass spectrometry confirmed the ligand exchange, the ^1H NMR spectrum of the crude product was unexpectedly complex. Closer inspection of the thin layer chromatograph of the reaction mixture revealed two products with very similar R_f values in a ratio of approximately 2:3. Despite their proximity, these proved amenable to separation by preparative thin-layer chromatography on silica gel-coated plates (CH_2Cl_2:MeOH, 98.5:1.5 as eluent).

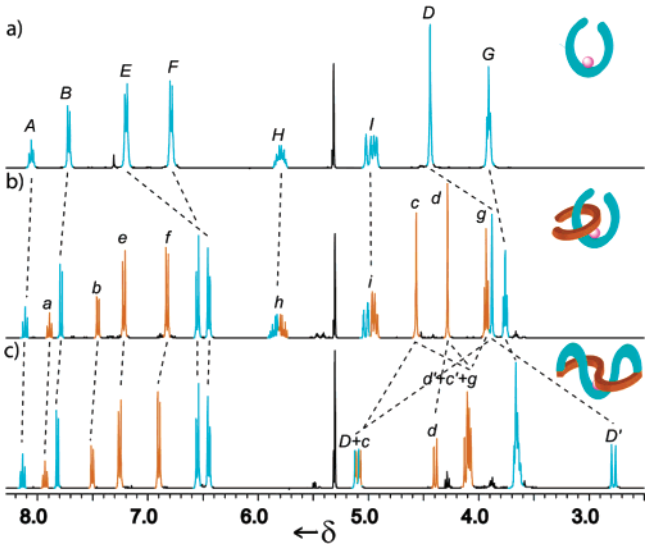

Figure 1. ^{1}H NMR spectra (400 MHz, 19:1 CD_2Cl_2:CD_3CN, 298 K) of (a) **L1**Pd(CH_3CN), (b) **L1**Pd**L2**, and (c) **L3**Pd. The lettering refers to the assignments shown in Scheme 3.

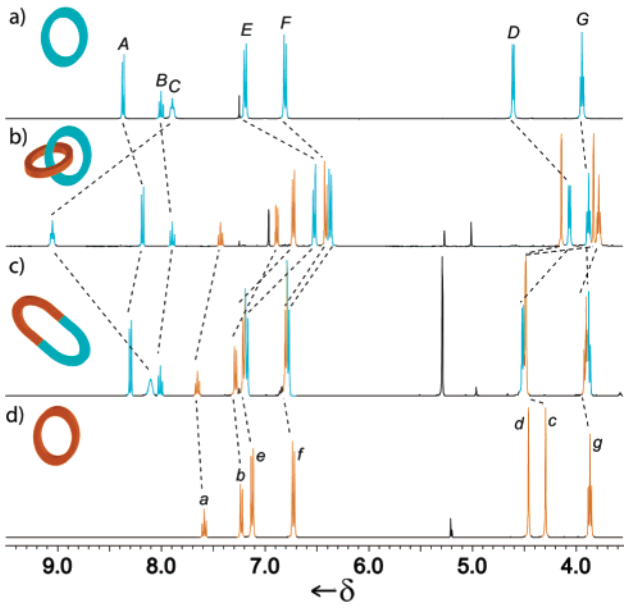

Figure 2. ^{1}H NMR spectra (400 MHz, $CDCl_3$, 298 K) of (a) H_2**L4**, (b) H_2**L6**, (c) H_2**L3**, and (d) **L**5. The lettering refers to the assignments shown in Scheme 3.

The isolated complexes gave indistinguishable fragmentation patterns by electrospray ionization mass spectrometry, the molecular mass ion suggesting they were both isomers of **L4**Pd**L2**. However, the ^{1}H NMR spectra exhibited important differences between the two products. When compared to the spectra of the starting materials, the minor isomer (lower R_f, Figure 4d) showed significant shielding of the **L4** benzyl rings (H_E and H_F), indicative of aromatic stacking with the pyridine group of **L2**. In contrast, the major isomer (higher R_f, Figure 4b) showed no evidence of stacking interactions but a greater degree of complexity in both the **L2** signals (two sets of nonequivalent H_b, H_c, H_d, H_e, and H_f resonances) and the H_D methylene groups (an AB system with a 2.5 ppm separation between the two proton environments) of **L4**. From this, we tentatively assigned the two products as "threaded" (minor isomer) and "threaded" (minor isomer) atropisomers,[21] **L4**Pd(*exo*-**L2**) and **L4**Pd(*endo*-**L2**), respectively (Scheme 3).

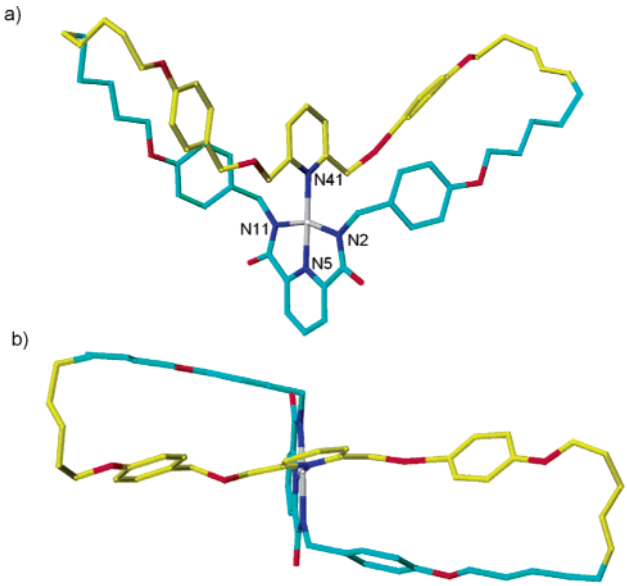

Figure 3. X-ray crystal structure of "figure-of-eight" complex **L3**Pd grown by slow cooling of a warm, saturated solution of the complex in acetonitrile. (a) Side-on and (b) top views. Carbon atoms originating from **L1** are shown in light blue, those from **L2** in yellow. Oxygen atoms are red, nitrogen dark blue, palladium gray. Selected bond lengths [Å]: Pd−N2 2.015, Pd−N5 1.941, Pd−N11 2.027, Pd−N41 2.052; tridentate fragment bite angle [°]: N2−Pd−N11 161.0.

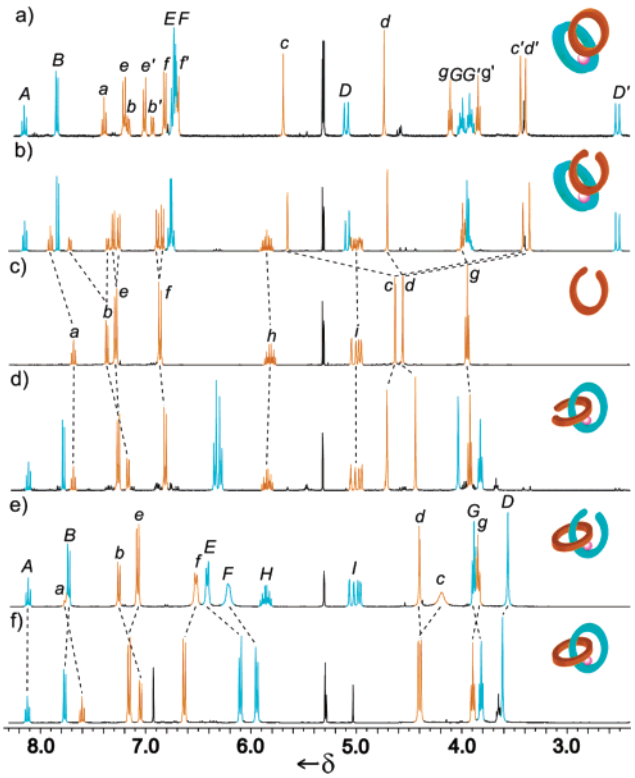

Figure 4. ^{1}H NMR spectra (400 MHz, CD_2Cl_2, 298 K) of (a) **L4**Pd**L5**, (b) **L4**Pd(*exo*-**L2**), (c) **L2**, (d) **L4**Pd(*endo*-**L2**), (e) **L1**Pd**L5**, and (f) **L6**Pd. The lettering refers to the assignments shown in Scheme 3.

Intriguingly, CPK models suggested that cyclization of **L2** could occur with *each* atropisomer of **L4**Pd**L2**, suggesting that two compounds of identical connectivity but different conformations[22] are predisposed to form topological isomeric products

upon RCM—the [2]catenate, **1**, and the analogous noninterlocked double macrocycle structure, **3**. Sure enough, treatment of the 2:3 mixture of atropisomers with Grubbs' catalyst in CH_2Cl_2, followed by hydrogenation and demetalation (Scheme 3, vii (three steps—the mixtures of topological and olefin isomers preventing the isolation of pure products until the end of the reaction sequence)), afforded three products: macrocycles H_2**L4** and **L5** arising from complex **3**, and a further compound, which mass spectrometry confirmed to be a different isomer of H_2**L3**, in 25% overall yield for the three steps.[23]

^{1}H NMR spectroscopy of the new compound in $CDCl_3$ (Figure 2b) revealed shielding of most resonances compared to the free macrocycles H_2**L4** (Figure 2a) and **L5** (Figure 2d) characteristic of interdigitation, suggesting that it was indeed the [2]catenand H_2**L6**. The exception to the upfield trend in shifts was the amide protons (H_C), which were shifted significantly downfield (ca. 1.3 ppm) in the catenand compared to those of H_2**L4**, indicative of a significant hydrogen-bonding interaction between the amide protons of one ring and the pyridine nitrogen of the other. In contrast, the analogous amide protons in the 58-membered free macrocycle H_2**L3** occur at 8.11 ppm in $CDCl_3$ (Figure 2c), only slightly downfield of their position in H_2**L4** (7.88 ppm, Figure 2a), meaning that little intramolecular hydrogen bonding is occurring in the large flexible macrocycle. Why is this internal hydrogen bonding absent when it is so clearly present in the mechanically bonded isomer H_2**L6**? First, the size and nature of the solvent-exposed surfaces of the compact [2]catenand structure and the large, relatively open, macrocycle must be very different, making desolvation of the amide and pyridine residues in the catenane a significantly less energetically costly process. Second, with the 2,6-bis(oxymethylene)pyridine and 2,6-pyridinecarboxamide groups on different components, the macrocycles in H_2**L6** can orientate themselves for inter-residue hydrogen bonding with little more than the loss of a single rotational degree of freedom. In contrast, alignment of the groups to enable a similar interaction within H_2**L3** would significantly restrict the number of conformations accessible by the alkyl chains in the large flexible ring, the resulting losses in degrees of freedom raising the energy of the hydrogen-bonded structure. This unusual orthogonal double bifurcated bis-pyridine hydrogen-bonding interaction is also observed in the related [2]rotaxane system.[17]

Reintroduction of Pd(II) into the free ligand systems (H_2**L3** → **L3**Pd, Scheme 3, xii; H_2**L6** → **L6**Pd, Scheme 3, xiii; H_2**L4** → **L4**Pd(CH_3CN) + **L5** → **L4**Pd**L5**, Scheme 3, v, viii) proceeded smoothly in each case, the last two providing pure samples of complexes formed previously as intermediates during each pathway of the Route II syntheses. ESI mass spectrometry initially identified the formation of **L4**Pd**L5**, confirming that both macrocycles could simultaneously bind to palladium without being interlocked. ^{1}H NMR spectroscopy (Figure 4a) corroborated this result and showed significant similarity (a diastereotopic environment for H_D, and two sets of signals for each H_b, H_c, H_d, H_e, H_f, and H_g) to the presumed nonthreaded isomer of **L4**Pd**L2** (Figure 4b). These spectral features are consistent with orthogonal binding of the rings to the square planar geometry metal, with neither macrocycle being able to pass through the cavity of the other nor rotate (at least not rapidly on the NMR time scale in the case of the monodentate ligand) about the plane of the square planar coordination geometry. This means both macrocycles are perforce desymmetrized in the plane that they coordinate to the metal, that is, top from bottom in **L4** and left from right in **L5** (as **L4**Pd**L5** is depicted in Figure 5a).

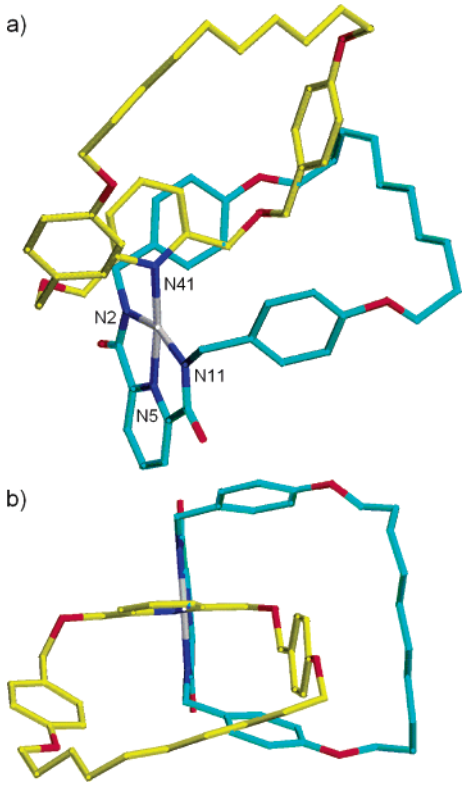

Figure 5. X-ray crystal structure of noninterlocked double macrocycle complex **L4**Pd**L5** grown from a saturated solution of the complex in acetone. (a) Side-on and (b) top views. Carbon atoms of the **L4** macrocycle are shown in light blue, and those of the **L5** macrocycle in yellow; oxygen atoms are red, nitrogen dark blue, and palladium gray. Selected bond lengths [Å]: N2—Pd 2.032, N5—Pd 1.943, N11—Pd 2.032, N41—Pd 2.077; tridentate fragment bite angle [°]: N2—Pd—N11 160.8.

Pleasingly, the pure samples of **L4**Pd**L5** and **L6**Pd both provided single crystals suitable for structure elucidation by X-ray crystallography (Figure 5 and Figure 6, respectively). Between them, the X-ray crystal structures of **L3**Pd, **L4**Pd**L5**, and **L6**Pd confirm not only the identity of the metal complexes—a unique set of topological (**L4**Pd**L2** and **L6**Pd) and constitutional (**L3**Pd and **L4**Pd**L5**/**L6**Pd) isomers—but also the structural assignments of the free ligands inferred by the earlier ^{1}H NMR and mass spectrometry analysis.

Atropisomer-Specific Synthesis of Different Topological Isomers. Although RCM (and subsequent hydrogenation and demetalation) of the mixture of the two **L4**Pd**L2** atropisomers gives a ratio of isolated interlocked to noninterlocked products similar to the starting atropisomer ratio, it does not necessarily follow that one atropisomer leads solely to one product. The

(21) The term "atropisomerism" technically refers to conformers which can be isolated as separate chemical species as a result of restricted rotation about a single bond [IUPAC Compendium of Chemical Terminology 2nd ed.; 1997]. We stretch this definition slightly in applying it to **L4**Pd(*endo*-**L2**) and **L4**Pd(*exo*-**L2**), which are isolable as a result of restricted rotation about various single bonds in particular ligand orientations.

(22) The term "co-conformation" is generally used to refer to the relative positions of mechanically interlocked components with respect to each other [Fyfe, M. C. T.; Glink, P. T.; Menzer, S.; Stoddart, J. F.; White, A. J. P.; Williams, D. J. *Angew. Chem., Int. Ed. Engl.* **1997**, *36*, 2068—2070]. However, since the two components in **L4**Pd(*endo*-**L2**) and **L4**Pd(*exo*-**L2**) are connected by a continuous sequence of covalent and coordination bonds, in this case "conformation" is a sufficient descriptor.

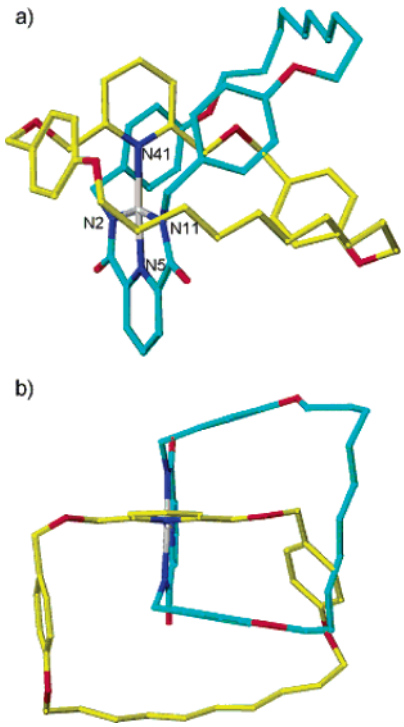

Figure 6. X-ray crystal structure of palladium[2]catenate **L6**Pd grown by slow cooling of a warm, saturated solution of the complex in acetonitrile. (a) Side-on and (b) top views. Carbon atoms of the **L4** macrocycle are shown in light blue, and those of the **L5** macrocycle in yellow; oxygen atoms are red, nitrogen dark blue, and palladium gray. Selected bond lengths [Å]: Pd−N2 1.934, Pd−N5 2.041, Pd−N11 2.036, Pd−N41 2.079; tridentate fragment bite angle [°]: N2−Pd−N11 160.2.

interconversion of the two **L4**Pd**L2** atropisomers in solution was investigated by ^{1}H NMR spectroscopy. The initial threaded:nonthreaded ratio of ca. 2:3 remained unchanged over 7 days in CD_2Cl_2 at room temperature. Similarly, spectra of pure samples of each of the compounds were invariant under these conditions, demonstrating that the atropisomers are kinetically stable at room temperature in a noncoordinating solvent. However, addition of ∼10% CD_3CN to either of the pure atropisomer solutions or the 2:3 mixture led to a gradual change in the threaded:nonthreaded ratio, increasing to ca. 7:3 after 4 days. This suggests that the threaded isomer is thermodynamically favored, and that atropisomer interconversion can take place via the dissociation of **L2** from either form of **L4**Pd**L2**, the vacant coordination site being temporarily filled by a molecule of CD_3CN. Accordingly, the reaction between **L2** and **L4**Pd(CH_3CN) was repeated in refluxing acetonitrile. After several hours, ^{1}H NMR spectroscopy showed a 7:3 ratio of the threaded:nonthreaded forms of **L4**Pd**L2**. Heating over 2 days increased the ratio to 8:1, after which no further change occurred.

RCM of single atropisomer samples of **L4**Pd**L2** in CH_2Cl_2 did, indeed, generate a single new species in each case. The product of RCM of the presumed **L4**Pd(*endo*-**L2**) complex was hydrogenated to give solely the [2]catenate, **L6**Pd; the product of RCM of presumed **L4**Pd(*exo*-**L2**) proved unstable to hydrogenation,[23] so the metal was removed instead (KCN, MeOH, CH_2Cl_2, 20 °C, 1 h and then 40 °C, 0.5 h), liberating two different macrocycles, H_2**L4** (96%) and the unsaturated olefin analogue of **L5** (93%).

Route III: Metal-Directed RCM of L1. Finally, we investigated the product distribution arising from preforming the monodentate macrocycle and applying metal-directed cyclization of the tridentate ligand (Scheme 3, Route III).[24] **L1**Pd(CH_3CN) and **L5** were stirred together in dichloromethane at room temperature (Scheme 3, ix) and, in contrast to the analogous step in Route II, reacted to give a single product rather than a mixture of atropisomers. The ^{1}H NMR spectrum of **L1**Pd**L5** (Figure 4e) suggests the two ligands are threaded; the upfield shift of H_E and H_F compared to similar protons in the nonthreaded **L4**Pd**L5** and **L4**Pd(*exo*-**L2**) complexes (Figure 4a and b, respectively), indicating π-stacking of the benzyl groups of **L1** with the pyridine unit of **L5**. It is difficult to distinguish between whether **L1**Pd**L5** can exist as threaded/nonthreaded atropisomers but is formed solely as the (*exo*-**L1**)Pd**L5** isomer, or rather threaded and nonthreaded forms of **L1**Pd**L5** are in equilibrium with the threaded conformation being thermodynamically preferred by several kcal mol^{-1}. In any event, RCM of **L1**Pd**L5** and subsequent hydrogenation (Scheme 3, x) afforded exclusively the [2]catenate, **L6**Pd, in 78% yield, making this route both synthetically efficient and completely selective for the mechanically interlocked topological isomer.

Conclusions

A [2]catenate and the isomeric single macrocycle and double macrocycle metal complexes can each be efficiently assembled about a palladium(II) template via RCM. The order in which the tridentate and monodentate ligand cyclization reactions and coordination steps are performed determines the outcome of the synthetic pathway, providing selective routes to each of the three topological and constitutional isomers. In one case, preforming the tridentate macrocycle followed by its coordination along with the acyclic monodentate ligand to the Pd produces threaded and nonthreaded atropisomers. These can be isolated and, while the individual forms are stable in dichloromethane, they can be interconverted in a coordinating solvent through ligand exchange. Each atropisomer was shown to be a true intermediate to a different topological product, meaning that, in this reaction, the choice of solvent can determine whether the [2]catenate is formed or its noninterlocked isomer. It is remarkable to see how topology and connectivity can be selected so exquisitely—in three different forms—using just one set of organic building blocks and a metal atom with a two-dimensional coordination geometry.

Experimental Section

Selected Spectroscopic Data for the Set of Three Constitutional and Topological Isomers. L3 Pd: ^{1}H NMR (400 MHz, CD_2Cl_2, 298 K): δ = 1.09−1.84 (m, 32H, alkyl-H), 2.70 (d, 2H, J = 14.4 Hz, $H_{D'}$), 3.64 (m, 4H, H_G), 4.00−4.13 (m, 8H, $H_g + H_{c'} + H_{d'}$), 4.39 (d, 2H, J = 10.6 Hz, H_d), 5.04−5.14 (m, 4H, $H_c + H_D$), 6.38 (d, 4H, J = 8.6 Hz, H_E), 6.49 (d, 4H, J = 8.6 Hz, H_F), 6.84 (d, 4H, J = 8.6 Hz,

(23) The hydrogenation conditions employed in Routes I and III led to a complex mixture when applied to the products of metathesis in Route II. Not only was significant decomplexation of the somewhat strained noninterlocked double macrocycle complex observed but also the resulting free monodentate ligand, **L5**, was degraded, presumably by hydrogenolysis of the benzyl ether moieties. Although the use of Pd EnCat did not prevent the ligand decomplexation during the hydrogenation step, it significantly reduced the degradation of the free monodentate macrocycle [Bremeyer, N.; Ley, S. V.; Ramarao, C.; Shirley, I. M.; Smith, S. C. *Synlett* **2002**, 1843−1844].

(24) Leigh, D. A.; Lusby, P. J.; Slawin, A. M. Z.; Walker, D. B. Submitted for publication.

H_f), 7.20 (d, 4H, J = 8.6 Hz, H_e), 7.45 (d, 2H, J = 7.8 Hz, H_b), 7.76 (d, 2H, J = 7.8 Hz, H_B), 7.88 (t, 1H, J = 7.8 Hz, H_a), 8.08 (t, 1H, J = 7.8 Hz, H_A). ^{13}C NMR (100 MHz, CD_2Cl_2, 293 K): δ = 23.7, 25.2, 25.5, 27.5, 27.5, 27.5, 28.6, 29.5, 48.5, 67.1, 68.1, 71.8, 73.2, 114.0, 114.8, 121.2, 124.8, 128.5, 128.7, 129.5, 132.8, 139.1, 140.7, 152.8, 158.1, 158.6, 160.6, 171.1. HRMS (FAB, NOBA): Calcd for $C_{62}H_{75}N_4O_8$-Pd $[M + H]^+$ 1109.46169. Found 1109.46275. **L4**Pd**L5**: ^{1}H NMR (400 MHz, CD_2Cl_2, 298 K): δ = 0.81−1.74 (m, 32H, alkyl-H), 2.50 (d, 2H, J = 14.8 Hz, $H_{D'}$), 3.34−3.44 (m, 4H, $H_{d'} + H_{c'}$), 3.78−4.02 (m, 6H, $H_{g'} + H_{G'} + H_G$), 4.09 (t, 2H, J = 6.3 Hz, H_g), 4.72 (s, 2H, H_d), 5.08 (d, 2H, J = 14.8 Hz, H_D), 5.67 (s, 2H, H_c), 6.64−6.84 (m, 12H, $H_{f'} + H_F + H_E + H_f$), 6.92 (d, 1H, J = 7.8 Hz, $H_{b'}$), 6.99 (d, 2H, J = 8.6 Hz, $H_{e'}$), 7.12−7.22 (m, 3H, $H_b + H_e$), 7.38 (t, 1H, J = 7.8 Hz, H_a), 7.83 (d, 2H, J = 7.8 Hz, H_B), 8.13 (t, 1H, J = 7.8 Hz, H_A). ^{13}C NMR (100 MHz, CD_2Cl_2, 298 K): δ = 25.6, 25.9, 25.9, 28.5, 29.0, 29.1, 29.3, 29.4, 29.4, 29.6, 29.8, 29.9, 49.2, 67.8, 67.9, 68.3, 72.1, 72.8, 73.4, 76.3, 114.8, 114.9, 115.4, 122.0, 122.7, 125.1, 128.3, 129.9, 130.3, 130.5, 131.4, 133.0, 138.4, 141.3, 153.0, 158.2, 158.7, 159.6, 160.6, 161.9, 171.6. LRMS (ESI) m/z = 1132 $[M + Na]^+$. **L6**Pd: ^{1}H NMR (400 MHz, CD_2Cl_2, 293 K): δ = 1.04−1.50 (m, 24H, alkyl-H), 1.60 (m, 4H, alkyl-H), 1.70 (m, 4H, alkyl-H), 3.60 (s, 4H, H_D), 3.81 (t, 4H, J = 6.3 Hz, H_G), 3.89 (t, 4H, J = 6.3 Hz, H_g), 4.36−4.42 (m, 8H, $H_d + H_c$), 5.94 (d, 4H, J = 8.6 Hz, H_F), 6.10 (d, 4H, J = 8.6 Hz, H_E), 6.63 (d, 4H, J = 8.6 Hz, H_f), 7.05 (d, 2H, J = 7.8 Hz, H_b), 7.15 (d, 4H, J = 8.6 Hz, H_e), 7.60 (t, 1H, J = 7.8 Hz, H_a), 7.76 (d, 2H, J = 7.6 Hz, H_B), 8.13 (t, 1H, J = 7.6 Hz, H_A). ^{13}C NMR (100 MHz, CD_2Cl_2, 293 K): δ = 25.8, 26.0, 28.5, 28.7, 28.9, 29.2, 30.0, 30.1, 49.4, 67.1, 67.7, 69.6, 72.9, 114.5, 114.8, 121.2, 124.5, 128.2, 128.6, 131.7, 132.9, 138.8, 140.6, 153.1, 157.4, 159.5, 160.0, 171.1. HRMS (FAB, NOBA): Calcd for $C_{62}H_{75}N_4O_8$ Pd $[M + H]^+$ 1109.46169. Found 1109.46152.

Acknowledgment. This work was supported by the European Union Future and Emerging Technology program, *MechMol*, and the EPSRC.

Supporting Information Available: Experimental procedures and spectroscopic data for all new compounds, and thermal ellipsoids for the crystal structures of **L3**Pd, **L4**Pd**L5**, and **L6**Pd. This material is available free of charge via the Internet at http://pubs.acs.org.

JA053005A